Quantum dense coding network using multimode squeezed states of light

Ayan Patra,[1] Rivu Gupta,[1] Saptarshi Roy,[2] Tamoghna Das,[3] and Aditi Sen(De)[1]
[1]*Harish-Chandra Research Institute, A CI of Homi Bhabha National Institute, Chhatnag Road, Jhunsi, Prayagraj 211019, India*
[2]*Quantum Information and Computation Initiative, Department of Computer Science, The University of Hong Kong, Pokfulam Road, Hong Kong*
[3]*International Centre for Theory of Quantum Technologies, University of Gdańsk, 80-952 Gdańsk, Poland*

(Received 23 June 2022; accepted 4 October 2022; published 14 November 2022)

We present a framework of a multimode dense coding network with multiple senders and a single receiver using continuous variable systems. The protocol is scalable to arbitrary numbers of modes with the encoding being displacements while the decoding involves homodyne measurements of the modes after they are combined in a pairwise manner by a sequence of beam splitters, thereby exhibiting its potentiality to implement in laboratories with currently available resources. We compute the closed form expression of the dense coding capacity for the cases of two and three senders that involve sharing of three- and four-mode states, respectively. The dense coding capacity is computed with the constraint of fixed average energy transmission when the modes of the sender are transferred to the receiver after the encoding operation. In both the cases, we demonstrate the quantum advantage of the protocol using paradigmatic classes of three- and four-mode states. The quantum advantage increases with the increase in the amount of energy that is allowed to be transmitted from the senders to the receiver.

DOI: 10.1103/PhysRevA.106.052607

I. INTRODUCTION

Nonclassical correlations play a crucial role in building quantum information technologies like quantum cryptography [1–7], dense coding (DC) [8–12], teleportation [13–15], one-way quantum computation [16–22], and random number generation [23,24], to name a few. Among them, the dense coding protocol is essential for transmitting classical information without security from one place to another with the help of a shared entangled state, which exhibits improvements in capacity over its classical counterparts. The original DC proposal with point-to-point communication was later extended to multiparty networks involving multiple senders and a single as well as two receivers [25–29], although such design of networks is mostly limited to finite-dimensional systems (cf. [30,31]). Interestingly, it was shown that, even in the case of quantum key distribution, it is beneficial to apply the secure dense coding protocol as it doubles the rate of secure key per transmitted qubit between the honest parties, and also increases the chance of detecting the presence of a malicious eavesdropper up to two senders in the single-receiver scenario [32–34].

Continuous variable (CV) systems provide an important platform for realizing quantum protocols. It can overcome several limitations arising in the finite-dimensional case, a prominent one being the distinction of four orthogonal Bell states with linear optical elements required in the stage of decoding of classical information [35–39]. However, these drawbacks can be overcome when one considers CV systems, in particular, the mode-entanglement of multiphoton quantum optical systems, where the average number of photons in a mode is taken to be arbitrary. The pioneering work on dense coding in the field of CV systems (which we refer to as CVDC) was first proposed by Braunstein and Kimble [40] in which the Einstein-Podolsky-Rosen (EPR) state [41] is shared between a single sender and a single receiver to transfer classical information. The encoding operation is performed by applying the displacement operator, which is distributed according to a Gaussian distribution of vanishing mean and variance σ. In recent years, many developments have been made for the successful realization of classical information transmission in CV systems [42,43], particularly with shared Gaussian entangled states between the sender and the receiver [44–48].

In this paper, we design a framework for the dense coding protocol, involving an arbitrary number of senders and a single receiver, with quantum optical fields. Each of the senders performs local unitary encoding with the help of the displacement operator, drawn uniformly from a Gaussian distribution with variance σ. Thereafter, the modes are transmitted to the receiver, who combines the modes pairwise with the help of the beam splitters for decoding the message sent by the sender. The transmission coefficients of the beam splitters were kept arbitrary, so as to determine the decoding configuration which can overcome the classical bound. The proposed procedure works with an arbitrary number of senders and a single receiver.

When two and three senders share three- and four-mode genuinely entangled Gaussian states with a single receiver, respectively, we exhibit quantum advantage, i.e., when the capacity of the quantum protocol beats the classical threshold value for a given energy, which can be obtained between the

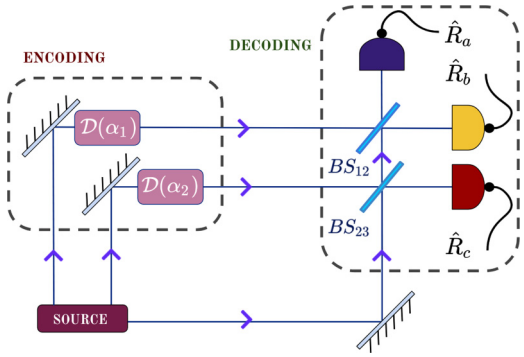

FIG. 1. Schematic diagram for the CVDC protocol involving two senders and a single receiver. The schematic has two components in DC: encoding at the senders' ends, which involve the displacement operators, denoted by $D(\alpha_k)$ $(k = 1, 2)$, and the decoding part in the receiver's side after obtaining modes from the sender upon encoding. The second one requires a combination of beam splitters, BS_{12}, and BS_{23} and homodyne measurements of quadratures, $\hat{R}_a$, $\hat{R}_b$, and $\hat{R}_c$ at the receiver's end.

arbitrary number of senders and a receiver without any shared entanglement. Specifically, we identify the region characterized by the state parameters which lead to quantum advantage. The DC protocol in CV systems, required to obtain a valid classical capacity, is typically implemented with a fixed average number of photons in the sender modes, which bounds the energy of the system. We report here the threshold photon number necessary for outperforming the classical routine. Moreover, the initial squeezing strength leading to a quantum benefit is determined for some classes of paradigmatic three- and four-mode states, which manifest that the current state of the art experiments can achieve quantum advantage in a DC network.

The paper is organized in the following way. The multimode dense coding scenario is introduced in Sec. II which includes the encoding and decoding of classical information, the capacity of DC via quantum protocol, and the corresponding classical scheme without the shared entangled state. We then illustrate the DC capacities when the senders and a receiver share three- and four-mode channels in Secs. III and IV, respectively. The comparisons of DC capacities with classical protocols are also discussed in these sections, while concluding remarks are in Sec. V.

II. FRAMEWORK FOR MULTIMODE DENSE CODING NETWORK

We now introduce the formalism of the multimode dense coding network involving multiple senders and a single receiver necessary for our investigation (see Fig. 1 for the case of two senders and a single receiver). We start by briefly recapitulating the basic properties of Gaussian states and describe how they can be characterized by their first two moments in the phase-space formalism. We also elucidate on the Wigner function formalism, which turns out to be useful in the study of DC in continuous variable systems and present the dense coding routine for classical information transfer between multiple senders and a single receiver. We focus on the multimode entangled states, which are necessary for successful implementation of the process and move on to construct the encoding and decoding schemes to arrive at an expression for the multimode dense coding capacity. Finally, we derive the classical capacity for multisender dense coding using continuous variable states without entanglement, which sets a benchmark on the classical bound for accessing the quantum advantage of the protocol.

A. Multimode Gaussian states as resources

Gaussian states are completely characterized by their displacement vector $\mathbf{d}$ and covariance matrix Ξ [44], given by

$$d_i = \langle \hat{R}_i \rangle, \tag{1}$$

and

$$\Xi_{ij} = \tfrac{1}{2}\langle \hat{R}_i \hat{R}_j + \hat{R}_j \hat{R}_i \rangle - \langle \hat{R}_i \rangle \langle \hat{R}_j \rangle, \tag{2}$$

where $\hat{R}_i$s are the phase-space quadrature operators, $\hat{\mathbf{R}} = (\hat{q}_1, \hat{p}_1, \ldots, \hat{q}_{\mathcal{N}}, \hat{p}_{\mathcal{N}})^T$, satisfying the canonical commutation relation (CCR), $[\hat{R}_i, \hat{R}_j] = iJ_{kl}$. Here J is the $\mathcal{N}$-mode symplectic form $J = \bigoplus_{i=1}^{\mathcal{N}} \Omega$, where

$$\Omega = \begin{bmatrix} 0 & 1 \\ -1 & 0 \end{bmatrix}.$$

Therefore, the transformations which preserve the CCR are symplectic, i.e., $SJS^T = J$.

In the phase-space formalism of CV systems, the states can equivalently be characterized by the characteristic function [49], which reads, for an $\mathcal{N}$-mode state ρ, as

$$\chi_\rho(\boldsymbol{\alpha}) = \mathrm{Tr}[\rho \hat{D}(\boldsymbol{\alpha})], \tag{3}$$

where $\boldsymbol{\alpha} = (\alpha_1, \alpha_2, \ldots, \alpha_{\mathcal{N}})$ and $\hat{D}(\boldsymbol{\alpha}) = \bigotimes_{i=1}^{\mathcal{N}} \hat{D}(\alpha_i)$ with $\hat{D}(\alpha_k) = \exp(\alpha_k \hat{a}_k^\dagger - \alpha_k^* \hat{a}_k)$ being the displacement operator for mode k. The Fourier transform of the characteristic function is the well-known Wigner function [50], which for an $\mathcal{N}$-mode Gaussian state, turns out to be a $2\mathcal{N}$-variable Gaussian function, given by [44]

$$W(\mathbf{R}) = \frac{\exp[-\frac{1}{2}(\mathbf{R}-\mathbf{d})^T \Xi^{-1} (\mathbf{R}-\mathbf{d})]}{(2\pi)^{\mathcal{N}} \sqrt{\det(\Xi)}}. \tag{4}$$

Operationally, the reduced Wigner function obtained by integrating over the quadrature variables of m modes gives the marginal probability distribution for the rest of the modes.

B. Elements of CV dense coding with multiple senders

Let us present here important constituents of the DC network with CV systems. One of the main ingredients of the prescribed protocol involving multiple senders and a single receiver is the class of the $(\mathcal{N}-1)$-parameter family of $\mathcal{N}$-mode Gaussian states shared between $(\mathcal{N}-1)$ senders and a single receiver. To implement successful DC, we require suitable encoding of classical information by the senders and the corresponding decoding procedure by the receiver after all the modes have been transferred to the receiver. The success

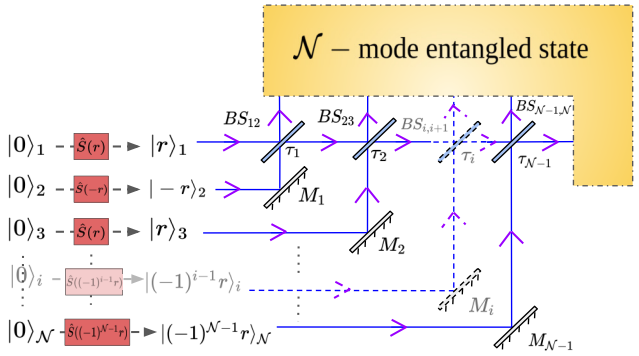

FIG. 2. Schematics to generate an $\mathcal{N}$-mode entangled state to be used for dense coding between $\mathcal{N}-1$ senders and a single receiver. Initially, we start with an $\mathcal{N}$-mode vacuum state denoted as $|0\rangle_1|0\rangle_2\ldots|0\rangle_{\mathcal{N}}$. Each mode is squeezed by a degree r, with alternate modes being squeezed in different quadratures. Specifically, modes undergoing momentum squeezing are denoted as $|r\rangle$ and are prepared by acting $S(r)$ on the initial vacuum mode while modes squeezed in the position quadrature are denoted as $|(-1)^{i-1}r\rangle$, which are prepared by acting $S[(-1)^{i-1}r]$ on the vacuum mode. Further, the modes are combined pairwise using beam splitters, i.e., modes i and $i+1$ are combined using $BS_{i,i+1}$ of transmittivity τ_i. This results in the $\mathcal{N}$-mode entangled state. In the figure, M_is represent mirrors.

of the protocol can be measured by computing the multimode dense coding capacity. The quantum advantage of the protocol can only be guaranteed when the DC capacity crosses the classical threshold on the capacity for a multimode channel.

1. Shared states between multiple senders and a receiver

We consider an $(\mathcal{N}-1)$-parameter family of $\mathcal{N}$-mode entangled states for the DC network between $(\mathcal{N}-1)$ senders, denoted as $\mathcal{S}_1, \mathcal{S}_2, \ldots, \mathcal{S}_{\mathcal{N}-1}$, and a single receiver $\mathcal{R}$. We now briefly mention a preparation procedure of such states starting from single-mode squeezed states and linear optical elements, namely, the beam splitters. In particular, we start from $\mathcal{N}$ single-mode squeezed states of identical squeezing strengths r but with alternately squeezed quadratures. These modes are entangled by the pairwise action of $(\mathcal{N}-1)$ beam splitters with transmission coefficients, $\tau_1, \tau_2, \ldots,$ and $\tau_{\mathcal{N}-1}$ which leads to a family of $(\mathcal{N}-1)$-parameter genuinely multimode entangled states which serve as resources for distributed dense coding between $(\mathcal{N}-1)$ senders and a single receiver. The generation of the resource states is schematically depicted through Fig. 2. The entanglement between the senders and the receiver [in the $(\mathcal{N}-1):1$ bipartition] depends upon the values of the parameters τ_i and we will show that the dense coding capacity does so as well.

2. Encoding and decoding

The aim of the DC scheme is to transmit classical messages via an $\mathcal{N}$-mode entangled state, which is distributed between $(\mathcal{N}-1)$ senders and the lone receiver. In particular, the protocol allows us to transmit $\mathcal{N}$ real numbers (which constitutes the classical message) through this state. Suppose the sender i encodes the classical message α_i in his or her mode with the help of a suitable displacement operator $\hat{D}(\alpha_i)$. Note that the α_is are, in general, complex. Since we attempt to send only $\mathcal{N}$ real numbers, all but one chooses the $\{\alpha_i\}$ to be real. Without loss of generality, we assume that the first sender encodes messages in both his or her input quadratures, i.e., α_1 is chosen to be complex while the remaining senders encode a single message, i.e., a real number, which is in either the position or the momentum quadrature of the available mode. Thus, we have $\mathcal{N}$ encoded messages. Each sender encodes α_i from a Gaussian distribution of zero mean and standard deviation σ. Since local operations and classical communication (LOCC) is allowed between the senders, we can assume that the standard deviation is fixed among all the senders. The probability distribution of the input messages reads as

$$p(\alpha) = \frac{1}{(2\pi\sigma^2)^{\mathcal{N}/2}} \exp\Big[-\sum_{i=1}^{\mathcal{N}} \frac{\alpha_i^2}{2\sigma^2}\Big]. \tag{5}$$

Upon encoding, the senders' modes are transmitted to the receiver along a noiseless quantum channel. The receiver then applies $(\mathcal{N}-1)$ beam splitters to combine the modes in a pairwise manner to start the decoding process. Therefore, the decoding essentially comprises the action of $[\hat{B}_{(\mathcal{N}-1)\mathcal{N}}(\tau_{\mathcal{N}-1})\ldots\hat{B}_{23}(\tau_2)\hat{B}_{12}(\tau_1)]^\dagger$ on all the modes with $\hat{B}_{ij}$ being the action of the beam splitters combining the modes i and j. This is followed by the homodyne measurements of suitable quadratures, which is performed to estimate the messages encoded by the senders. The decoding process yields the conditional probability distribution $p(\beta|\alpha)$ where β stands for the messages interpreted by the receiver upon decoding. The unconditional probability distribution of the decoded messages is then computed as

$$p(\beta) = \int d^{\mathcal{N}}\alpha\, p(\beta|\alpha)p(\alpha), \tag{6}$$

and the mutual information quantifying the information achievable from the $\mathcal{N}$-mode states at the receiver's side is given by

$$\mathcal{I}(\mathcal{S}_1\ldots\mathcal{S}_{\mathcal{N}-1}:\mathcal{R}) = \int d^{\mathcal{N}}\alpha d^{\mathcal{N}}\beta\, p(\beta|\alpha)p(\alpha)\ln\Big[\frac{p(\beta|\alpha)}{p(\beta)}\Big]. \tag{7}$$

Maximizing Eq. (7) with respect to σ under the constraint that the total number of photons at the modes of $(\mathcal{N}-1)$ senders is fixed to $\bar{N}$, we obtain the capacity. We observe that for an $\mathcal{N}$-mode state, the total photon number of the senders' modes after encoding is given by

$$\bar{N} = (\mathcal{N}-1)\sinh^2 r + \mathcal{N}\sigma^2, \tag{8}$$

and the capacity of dense coding reads

$$C^{\mathcal{S}_1\ldots\mathcal{S}_{\mathcal{N}-1}:\mathcal{R}}(\tau_1\ldots\tau_{\mathcal{N}-1}) = \max_{\substack{\sigma \\ \sum_{i=1}^{\mathcal{N}-1}\bar{n}_i=\bar{N}}} \mathcal{I}(\mathcal{S}_1\ldots\mathcal{S}_{\mathcal{N}-1}:\mathcal{R}), \tag{9}$$

where the constraint involved in the maximization routine is $\sum_{i=1}^{\mathcal{N}-1}\bar{n}_i = \bar{N}$.

The mutual information is optimized when

$$\bar{N} = (\mathcal{N}-1)e^r \sinh r. \tag{10}$$

Choosing σ as $(\frac{\mathcal{N}-1}{2\mathcal{N}}\sinh 2r)^{1/2}$ by substituting Eq. (10) in Eq. (8) for a given $\mathcal{N}$-mode state with sender signal strength $\bar{N}$, we can find the classical capacity of the quantum channel.

3. Classical threshold

The advantage of a quantum protocol in dense coding is assured if its capacity surpasses that of the corresponding classically available scheme. Therefore, we need to set a benchmark with which the classical capacity of a quantum channel can be compared. According to Holevo's theorem, if a classical message, say α, taken from a probability distribution $p(\alpha)$ is to be transmitted via a quantum state $\hat{\rho}_\alpha$, the mutual information $\mathcal{I}(\mathcal{S}:\mathcal{R})$ between the sender $\mathcal{S}$ and the receiver $\mathcal{R}$ is bounded above by the Holevo quantity [51]

$$\mathcal{I}(\mathcal{S}:\mathcal{R}) \leqslant S(\hat{\rho}) - \int d^2\alpha\, p(\alpha) S(\hat{\rho}_\alpha) \leqslant S(\hat{\rho}), \tag{11}$$

where $S(\hat{\rho}) = -\mathrm{tr}(\hat{\rho}\ln\hat{\rho})$ is the von Neumann entropy of the density operator $\hat{\rho} = \int d^2\alpha\, p(\alpha)\hat{\rho}_\alpha$.

Considering a legitimate constraint of having a fixed mean number of photons $\bar{N}$ (which can be modulated), the required task is to find the configuration of a single-mode bosonic field to maximize the mutual information, $\mathcal{I}(\mathcal{S}:\mathcal{R})$. It was shown [52,53] that the optimal channel capacity via the classical protocol is achieved by photon counting measurement from an ensemble of number states having maximum entropy, i.e., $\sum_n P(n)\,|n\rangle\langle n|$ with $P(n) = \bar{N}^n(1+\bar{N})^{-(n+1)}$.

With this optimal configuration of a single-mode bosonic channel, the channel capacity for a single sender and a single receiver without entanglement is found to be [53]

$$C_{cl}^{\mathcal{S}:\mathcal{R}}(\bar{N}) = (1+\bar{N})\ln(1+\bar{N}) - \bar{N}\ln\bar{N}. \tag{12}$$

In a similar spirit, the capacity with $\mathcal{N}-1$ senders and a single receiver yields

$$C_{cl}^{\mathcal{S}_1\ldots\mathcal{S}_{\mathcal{N}-1}:\mathcal{R}}(\{\bar{N}_i\}) = \sum_i^{\mathcal{N}-1}[(1+\bar{N}_i)\ln(1+\bar{N}_i) - \bar{N}_i\ln\bar{N}_i], \tag{13}$$

where $\bar{N}_i$ is the mean photon number of the sender's mode i. Imposing the constraint of having a fixed mean photon number $\bar{N}$ at the senders' mode, where $\bar{N} = \sum_i^{(\mathcal{N}-1)}\bar{N}_i$, the capacity in the classical scenario where the entanglement between senders and a receiver is absent can be obtained by maximizing $C_{cl}^{\mathcal{S}_1\ldots\mathcal{S}_{\mathcal{N}-1}:\mathcal{R}}(\{\bar{N}_i\})$ over $\{\bar{N}_i\}$ with the constraint $\bar{N} = \sum_i^{(\mathcal{N}-1)}\bar{N}_i$. The condition for achieving the maximum capacity turns out to be $\bar{N}_i = \bar{N}/(\mathcal{N}-1)$ with an equal distribution of photons being taken at all senders' modes. Substituting $\bar{N}_i = \bar{N}/(\mathcal{N}-1)$ in Eq. (13), we obtain the expression for capacity in the classical case with an arbitrary number of senders and a single receiver as

$$C_{cl}^{\mathcal{S}_1\ldots\mathcal{S}_{\mathcal{N}-1}:\mathcal{R}} = (\mathcal{N}-1)\left[\left(1+\frac{\bar{N}}{\mathcal{N}-1}\right)\ln\left(1+\frac{\bar{N}}{\mathcal{N}-1}\right) - \frac{\bar{N}}{\mathcal{N}-1}\ln\frac{\bar{N}}{\mathcal{N}-1}\right]. \tag{14}$$

Comparing $C_{cl}^{\mathcal{S}_1\ldots\mathcal{S}_{\mathcal{N}-1}:\mathcal{R}}$ with the capacity obtained via a shared entangled state, we can confirm the quantum advantage, which we will demonstrate explicitly for the shared three- and four-mode states in the succeeding sections.

III. CLASSICAL CAPACITY FOR THREE-MODE CHANNEL INVOLVING TWO SENDERS AND A SINGLE RECEIVER

To derive the expression for the classical capacity between two senders, and a single receiver, $\mathcal{S}_1$, $\mathcal{S}_2$, and $\mathcal{R}$, respectively, a three-mode squeezed state is initially distributed among them. A three-mode genuinely multimode entangled state is, in general, prepared with the help of a tritter. The class of such states constitute a two-parameter family, characterized by the transmittivities τ_1 and τ_2 of two beam splitters, which comprise the tritter. The three-mode entangled state identified by its displacement vector and covariance matrix can be represented as

$$\mathbf{d}_0 = (0,0,0,0,0,0)^T, \tag{15}$$

$$\Xi_0 = \begin{pmatrix} \mathcal{A} & 0 & \mathcal{R} & 0 & \mathcal{T} & 0 \\ 0 & \mathcal{B} & 0 & -\mathcal{R} & 0 & -\mathcal{T} \\ \mathcal{R} & 0 & \mathcal{C} & 0 & -\mathcal{S} & 0 \\ 0 & -\mathcal{R} & 0 & \mathcal{D} & 0 & \mathcal{S} \\ \mathcal{T} & 0 & -\mathcal{S} & 0 & \mathcal{E} & 0 \\ 0 & -\mathcal{T} & 0 & \mathcal{S} & 0 & \mathcal{F} \end{pmatrix}, \tag{16}$$

where

$$\begin{aligned}
\mathcal{A} &= \tfrac{1}{2}e^{-2r}[(e^{4r}-1)\tau_1 + 1],\\
\mathcal{B} &= \tfrac{1}{2}[e^{-2r}\tau_1 + e^{2r}(1-\tau_1)],\\
\mathcal{C} &= \tfrac{1}{2}[\sinh 2r(1-2\tau_1\tau_2) + \cosh 2r],\\
\mathcal{D} &= \tfrac{1}{2}e^{-2r}[(e^{4r}-1)\tau_1\tau_2 + 1],\\
\mathcal{E} &= \tfrac{1}{2}\{\sinh 2r[1-2\tau_1(1-\tau_2)] + \cosh 2r\},\\
\mathcal{F} &= \tfrac{1}{2}e^{-2r}[1+\tau_1(e^{4r}-1)(1-\tau_2)],\\
\mathcal{R} &= \sqrt{\tau_1\tau_2(1-\tau_1)}\sinh 2r,\\
\mathcal{S} &= \tau_1\sqrt{\tau_2(1-\tau_2)}\sinh 2r,\\
\mathcal{T} &= \sqrt{\tau_1(1-\tau_1)(1-\tau_2)}\sinh 2r.
\end{aligned} \tag{17}$$

All the initial single-mode squeezed states are considered to have equal squeezing strength r. For $\tau_1 = 1/3$ and $\tau_2 = 1/2$, we obtain the well-known basset-hound state [54–56].

A. Encoding by the senders

Since the state comprises three modes, two senders can send, at most, three real numbers accurately. Without loss of generality, we assume that $\mathcal{S}_1$ sends two real numbers α_{1x} and α_{1y}, encoded through a suitable displacement operation $\hat{\mathcal{D}}_1(\alpha)$ where $\alpha_1 = \alpha_{1x} + i\alpha_{1y}$ while $\mathcal{S}_2$ chooses to send a single real number α_{2y} with the help of the displacement $\hat{\mathcal{D}}_2(\alpha_2)$ having $\alpha_2 = i\alpha_{2y}$. Both the senders resort to a Gaussian distribution of their respective real numbers, having the same standard deviation σ. The input probability distribution is then given

by

$$p(\alpha) = \frac{1}{2\pi\sigma^2}\exp\left(-\frac{|\alpha_1|^2}{2\sigma^2}\right)\frac{1}{\sqrt{2\pi}\sigma}\exp\left(-\frac{|\alpha_2|^2}{2\sigma^2}\right). \tag{18}$$

The encoding process gives rise to the displacement vector and covariance matrices, given by

$$\mathbf{d}_{en} = (\sqrt{2}\alpha_{1x}, \sqrt{2}\alpha_{1y}, 0, \sqrt{2}\alpha_{2y}, 0, 0)^T, \tag{19}$$

$$\Xi_{en} = \Xi_0. \tag{20}$$

B. Decoding by the receiver

After the encoding process, the senders send their respective modes to the receiver, and hence the receiver possesses the three-mode state. Towards recovering the classical information, two beam splitters are used to combine modes 1 and 2 as well as modes 2 and 3, through $[\hat{B}_{23}(\tau_2)\hat{B}_{12}(\tau_1)]^\dagger$. Such a decoding routine results in a three-mode state with the displacement vector and covariance matrix, respectively, as

$$\begin{aligned}\mathbf{d}_{\rm dec} = \big(&\sqrt{2\tau_1}\alpha_{1x}, \sqrt{2\tau_2(1-\tau_1)}\alpha_{2y} + \sqrt{2\tau_1}\alpha_{1y},\\ &\sqrt{2(1-\tau_1)}\alpha_{1x}, \sqrt{2(1-\tau_1)}\alpha_{1y} - \sqrt{2\tau_1\tau_2}\alpha_{2y},\\ &0, \sqrt{2(1-\tau_2)}\alpha_{2y}\big)^T,\end{aligned} \tag{21}$$

$$\Xi_{\rm dec} = {\rm diag}\big(\tfrac{1}{2}e^{2r}, \tfrac{1}{2}e^{-2r}, \tfrac{1}{2}e^{-2r}, \tfrac{1}{2}e^{2r}, \tfrac{1}{2}e^{2r}, \tfrac{1}{2}e^{-2r}\big). \tag{22}$$

The receiver requires to undertake a homodyne detection to measure p_1, x_2, and p_3 since these quantities have the lowest variance in $\Xi_{\rm dec}$. It results in the probability distribution of the output variables (conditioned on the input) as

$$\begin{aligned}p(\beta|\alpha) &= \int dx_1 dp_2 dx_3 W_{\rho_{\mathcal{S}_1\mathcal{S}_2\mathcal{R}}}(x_1, \beta_1, \beta_2, p_2 : x_3, \beta_3)\\ &= \frac{1}{\pi^{3/2}}[\exp\{3r - e^{2r}(\beta_2 - \alpha_{1x}\sqrt{2(1-\tau_1)})^2\}]\\ &\quad\times[\exp\{-e^{2r}[\beta_1\\ &\quad-\sqrt{2}(\alpha_{1y}\sqrt{\tau_1} + \alpha_{2y}\sqrt{\tau_2(1-\tau_1)})]^2\}]\\ &\quad\times[\exp\{-e^{2r}(\beta_3 - \alpha_{2y}\sqrt{2(1-\tau_2)})^2\}],\end{aligned} \tag{23}$$

where $W_{\rho_{\mathcal{S}_1\mathcal{S}_2\mathcal{R}}}$ is the Wigner function of the state after the modes are combined by the receiver using the beam splitter setup described above [30]. β_i $(i = 1, 2, 3)$ represent the homodyne outcomes obtained by the receiver upon measuring on the mode i. The unconditioned probability of the homodyne variables from Eq. (6) in this case reads

$$p(\beta) = \int d^2\alpha_1 d\alpha_2 p(\beta|\alpha)p(\alpha). \tag{24}$$

Using Eqs. (18) to (24), the mutual information corresponding to this channel can be computed as

$$\begin{aligned}\mathcal{I}(\mathcal{S}_1\mathcal{S}_2 : \mathcal{R}) &= \int d^3\beta d^2\alpha_1 d\alpha_2 p(\beta|\alpha)p(\alpha)\ln\left[\frac{p(\beta|\alpha)}{p(\beta)}\right]\\ &= \frac{1}{2}\ln[(4e^{2r}\sigma^2+1)(4e^{2r}\sigma^2(1-\tau_1)+1)]\\ &\quad+\frac{1}{2}\ln[(4e^{2r}\sigma^2\tau_1(1-\tau_2)+1)].\end{aligned} \tag{25}$$

Since the decoding scheme is fixed to homodyne detection, the dense coding capacity is obtained by maximizing Eq. (25) over the standard deviation of the encoding displacement operations subject to a fixed average photon number constraint. This condition can be represented as

$$\bar{n}_1 + \bar{n}_2 = 2\sinh^2 r + 3\sigma^2 = \bar{N}. \tag{26}$$

For a fixed $\bar{N}$, the mutual information is maximized when $\sigma^2 = \frac{1}{3}\sinh 2r$ and $r = (1/2)\ln(1+\bar{N})$, leading to the expression for the dense coding capacity

$$\begin{aligned}C^{\mathcal{S}_1\mathcal{S}_2:\mathcal{R}}(\tau_1,\tau_2) &= \max_{\substack{\sigma\\ \bar{n}_1+\bar{n}_2=\bar{\mathcal{N}}}} \mathcal{I}(\mathcal{S}_1\mathcal{S}_2 : \mathcal{R})\\ &= \tfrac{1}{2}\ln\big[\tfrac{1}{27}[2\bar{N}(\bar{N}+2)+3][2\bar{N}(\bar{N}+2)(1-\tau_1)+3][2\bar{N}(\bar{N}+2)\tau_1(1-\tau_2)+3]\big].\end{aligned} \tag{27}$$

Substituting various values of τ_1 and τ_2, we obtain the CVDC capacity for different states belonging to the two-parameter family. Notice that, although the basset-hound state obtained with $\tau_1 = 1/3$ and $\tau_2 = 1/2$ possesses the maximum genuine multimode entanglement in this set of states, we find that there exist states (obtained with other values of τ_1 and τ_2) which furnish a greater CV dense coding capacity than that obtained via the basset-hound state (cf. [28]). For example, with $\tau_1 = \tau_2 = 1/2$, the DC capacity takes the form as

$$C^{\mathcal{S}_1\mathcal{S}_2:\mathcal{R}}(1/2,1/2) = \tfrac{1}{2}\ln\big[\tfrac{1}{54}[\bar{N}(\bar{N}+2)+3][\bar{N}(\bar{N}+2)+6][2\bar{N}(\bar{N}+2)+3]\big], \tag{28}$$

which increases monotonically with the increase of $\bar{N}$ and for a given $\bar{N}$, we notice that $C^{\mathcal{S}_1\mathcal{S}_2:\mathcal{R}}(1/2,1/2) > C^{\mathcal{S}_1\mathcal{S}_2:\mathcal{R}}(1/3,1/2)$.

C. Quantum advantage in DC

To guarantee the quantum advantage, it is important to compare the classical capacity of a quantum channel with the capacity in a classical protocol. From Eq. (14), the optimum capacity in the classical case for a channel with mean photon number $\bar{N}$ shared between two senders and one receiver reduces to

$$C_{cl}^{\mathcal{S}_1\mathcal{S}_2:\mathcal{R}} = 2(1+\bar{N}/2)\ln(1+\bar{N}/2) - 2(\bar{N}/2)\ln(\bar{N}/2). \tag{29}$$

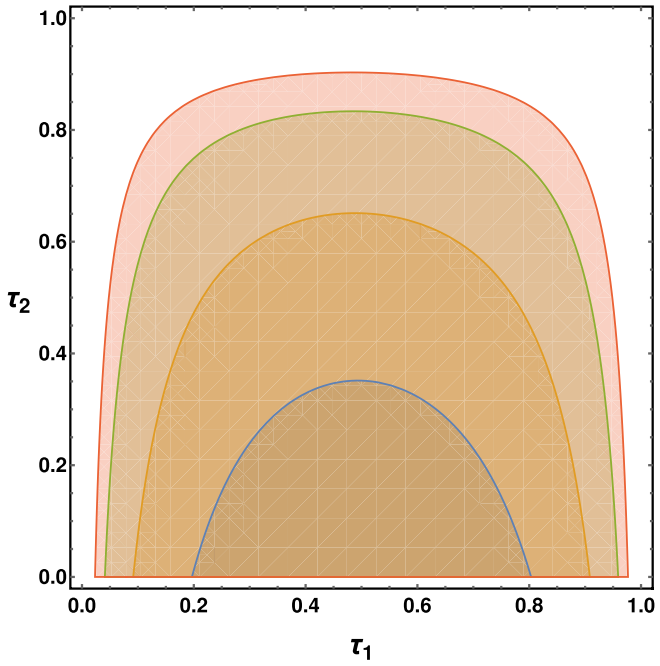

FIG. 3. Region plot of the state space bounded by τ_1 and τ_2 which provides quantum advantage of DC (in bits) having two senders and a single receiver with states belonging to the two parameter family of the three-mode states defined in the main text. The abscissa and ordinate represent τ_1 and τ_2, respectively. The blue, orange, green, and red curves (from below) correspond to $\bar{N} = 7$, $\bar{N} = 10$, $\bar{N} = 15$, and $\bar{N} = 20$. Note that all the states bounded by each curve can provide quantum advantage in DC. All the axes are dimensionless.

Let us define the quantum advantage in the DC network involving an arbitrary number of senders and a single receiver as

$$\Delta^{\mathcal{S}_1\mathcal{S}_2\cdots\mathcal{S}_{\mathcal{N}-1}:\mathcal{R}} = C^{\mathcal{S}_1\mathcal{S}_2\mathcal{S}_{\mathcal{N}-1}:\mathcal{R}}(\tau_1, \tau_2, \ldots, \tau_{\mathcal{N}-1}) - C_{cl}^{\mathcal{S}_1\mathcal{S}_2\cdots\mathcal{S}_{\mathcal{N}-1}:\mathcal{R}}, \quad (30)$$

for a fixed photon number. The positivity of the above ensures quantum advantage in the shared channels.

Let us identify the range of τ_1 and τ_2 for which the three-mode state provides quantum advantage, i.e., $\Delta^{\mathcal{S}_1\mathcal{S}_2:\mathcal{R}} > 0$ for a fixed $\bar{N}$ as illustrated in Fig. 3. We find that, with increasing $\bar{N}$, the region bounded in the (τ_1, τ_2) plane providing quantum advantage also grows in size. Furthermore, with $\tau_1 = 0.5$, we find the largest range of τ_2 which provides quantum advantage for a given $\bar{N}$. This indicates that states prepared with $\tau_1 = 0.5$ are more suitable for multimode DC between two senders and a lone receiver.

1. Threshold energy for quantum advantage

For any given values of τ_1 and τ_2, there exists a threshold energy, say, $\bar{N}_{th}^{\mathcal{S}_1\mathcal{S}_2:\mathcal{R}}(\tau_1, \tau_2)$, above which the quantum advantage can be achieved. Although it is very hard to find such an analytical expression of $\bar{N}_{\text{th}}^{\mathcal{S}_1\mathcal{S}_2:\mathcal{R}}(\tau_1, \tau_2)$, we can find the threshold energy numerically for a given τ_1 and τ_2 by solving the equation $C^{\mathcal{S}_1\mathcal{S}_2:\mathcal{R}}(\tau_1, \tau_2) = C_{cl}^{\mathcal{S}_1\mathcal{S}_2:\mathcal{R}}$ for $\bar{N}$. For example, we find the value of $\bar{N}_{\text{th}}^{\mathcal{S}_1\mathcal{S}_2:\mathcal{R}}(1/2, 1/2) = 8.15$, i.e., the three-mode entangled state having the state parameters $\tau_1 = \tau_2 = 1/2$ can offer a quantum advantage in the DC protocol at the minimum expense of energy $\bar{N}_{th}^{\mathcal{S}_1\mathcal{S}_2:\mathcal{R}}(1/2, 1/2) = 8.15$. For a given energy $\bar{N}$, we find that

$$\tau_1\big|_{\substack{\max\\\min}} = 0.5 \pm \frac{\sqrt{16[\bar{N}(\bar{N}+2)+3]^2 - \frac{27\bar{N}^{-2\bar{N}}(\bar{N}+2)^{2\bar{N}+4}}{2\bar{N}(\bar{N}+2)+3}}}{8\bar{N}(\bar{N}+2)}, \quad (31)$$

and for a given τ_1 and $\bar{N}$,

$$\tau_2\big|_{\max} = 1 + \frac{3}{2(\bar{N}^2\tau_1 + 2\bar{N}\tau_1)} - \frac{27\bar{N}^{-2\bar{N}-1}(\bar{N}+2)^{2\bar{N}+3}}{32\tau_1[2\bar{N}(\bar{N}+2)+3][2\bar{N}(\bar{N}+2)(1-\tau_1)+3]}, \quad (32)$$

where $\tau_i|_{\substack{\min\\\max}}$ represents the region bounded by τ_i which provides quantum advantage. Moreover, the minimum number of photons at the senders' mode required to avail the quantum advantage is then given by

$$\bar{N}_{th}^{\mathcal{S}_1\mathcal{S}_2:\mathcal{R}}\big|_{\min_{\{\tau_1,\tau_2\}}} = 5.38,$$

where minimization is performed over all possible values of τ_1 and τ_2.

2. Quantum advantage with large squeezing strength

Let us now investigate the ratio of classical capacity of a quantum channel and the capacity in the classical protocol for large-resource squeezing r. Substituting $\bar{N} = 2e^r \sinh r$ [see Eq. (10)] into Eq. (27), we obtain $C^{\mathcal{S}_1\mathcal{S}_2:\mathcal{R}} \sim 6r$, whereas the same substitution in Eq. (29) yields $C_{cl}^{\mathcal{S}_1\mathcal{S}_2:\mathcal{R}} \sim 4r$ for large r. Hence the ratio becomes

$$\frac{C^{\mathcal{S}_1\mathcal{S}_2:\mathcal{R}}}{C_{cl}^{\mathcal{S}_1\mathcal{S}_2:\mathcal{R}}} = \frac{3}{2} \quad \text{(at large } r\text{)}. \quad (33)$$

Knowing that the quantum protocol for $\tau_1 = \tau_2 = 1/2$ can overcome the classical threshold value when the total photon number of the senders' modes is $\bar{N} \geqslant 8.15$, we can find that the minimum squeezing required for quantum advantage in the two sender-one receiver scenario, denoted by $r_{\text{break-even}}^{\mathcal{S}_1\mathcal{S}_2:\mathcal{R}}(\tau_1 = 1/2, \tau_2 = 1/2)$, is 1.10685. Note, however, that $r_{\text{break-even}}^{\mathcal{S}_1\mathcal{S}_2:\mathcal{R}}(1/2, 1/2)$ is higher than that for the single sender-single receiver regime [40]. It is due to the fact that $C_{cl}^{\mathcal{S}_1\mathcal{S}_2:\mathcal{R}}$ is much higher than the classical bound for the DC protocol with a single sender-receiver duo.

IV. MULTIMODE DENSE CODING NETWORK WITH FOUR-MODE STATES

Akin to the case for three-mode channels, let us consider a general class of four-mode genuinely entangled Gaussian states, characterized by three parameters, τ_1, τ_2, and τ_3, shared between three senders $\mathcal{S}_i$, $(i = 1, 2, 3)$ and a receiver $\mathcal{R}$.

A. Encoding

Three senders, $\mathcal{S}_1, \mathcal{S}_2$, and $\mathcal{S}_3$, perform displacement operators on their respective modes as a part of the encoding process. The displacement amplitude for each sender is proportional to the message they wish to send. Like in the previous three-mode situation, we assume, without loss of generality, that $\mathcal{S}_1$ incorporates displacement in both the quadratures of his or her available mode with an amplitude $\alpha_1 = \alpha_{1x} + i\alpha_{1y}$. $\mathcal{S}_2$ chooses to displace only the momentum quadrature by α_{2y} while the position displacement α_{3x} is performed by $\mathcal{S}_3$. The input messages belong to a Gaussian ensemble characterized by the probability distribution

$$p(\alpha) = \frac{1}{(2\pi\sigma^2)^2} \exp\Big[-\frac{1}{2\sigma^2}\big(\alpha_{1x}^2 + \alpha_{1y}^2 + \alpha_{2y}^2 + \alpha_{3x}^2\big)\Big]. \tag{34}$$

The senders then transfer their modes, postencoding, to the receiver $\mathcal{R}$ via noiseless quantum channels.

B. Decoding

To decode the messages, the receiver combines all the four modes at his disposal, with the help of the beam splitter setup, represented as

$$[\hat{B}_{34}(\tau_3)\hat{B}_{23}(\tau_2)\hat{B}_{12}(\tau_1)]^\dagger.$$

The homodyne detection by the receiver on modes p_1, x_2, p_3, and x_4 leads to the conditional probability on the decoded message (here, the subscripts on the numbers indicate the quadrature on which the homodyne detection is performed), given by

$$\begin{aligned} p(\beta|\alpha) &= \int dx_1 dp_2 dx_3 dp_4 W_{\rho_{\mathcal{S}_1\mathcal{S}_2\mathcal{S}_3\mathcal{R}}}(x_1, \beta_1, \beta_2, p_2, x_3, \beta_3 : \beta_4, p_4) \\ &= \frac{1}{\pi}\exp(4r - e^{2r}\{[\beta_2 - \sqrt{2}(\alpha_{1x}\sqrt{1-\tau_1} - \alpha_{3x}\sqrt{\tau_1\tau_3(1-\tau_2)}]^2 + [\beta_1 - \sqrt{2}(\alpha_{1y}\sqrt{\tau_1} + \alpha_{2y}\sqrt{(1-\tau_1)\tau_2})]^2\}) \\ &\quad \times \frac{1}{\pi}\exp\{-e^{2r}[(\beta_3 - \sqrt{2}\alpha_{2y}\sqrt{1-\tau_2})^2 + (\beta_4 - \sqrt{2}\alpha_{3x}\sqrt{1-\tau_3})^2]\}. \end{aligned} \tag{35}$$

Here, $W_{\rho_{\mathcal{S}_1\mathcal{S}_2\mathcal{S}_3\mathcal{R}}}$ again represents the Wigner function of the state after the beam-splitter operation by the receiver and β_i are the homodyne outcomes for the mode, i. Following the same steps as in the case of the three-mode states, one can calculate the unconditioned decoding probability distribution $p(\beta)$ using Eq. (6), whereafter, the mutual information can be estimated as

$$\begin{aligned} &\mathcal{I}(\mathcal{S}_1\mathcal{S}_2\mathcal{S}_3 : \mathcal{R}) \\ &= \int d^4\beta d^2\alpha_1 d\alpha_2 d\alpha_3 p(\beta|\alpha)p(\alpha)\ln\Big[\frac{p(\beta|\alpha)}{p(\beta)}\Big] \\ &= \frac{1}{2}\ln\left[\sigma^8\left(e^{2r}4(1-\tau_1\tau_2) + \frac{1}{\sigma^2}\right)\left(\frac{(4e^{2r}\sigma^2+1)[4e^{2r}\sigma^2\tau_1(1-\tau_2)+1]}{\sigma^2(4e^{2r}\sigma^2(1-\tau_1\tau_2)+1)}\right)\left(\frac{1}{\sigma^2} + 4e^{2r}[\tau_1(1-\tau_2)\tau_3 + (1-\tau_3)]\right)\right] \\ &\quad + \frac{1}{2}\ln\Big[\frac{16e^{4r}\sigma^4(1-\tau_1)(1-\tau_3) + 4e^{2r}\sigma^2[\tau_1(1-\tau_2)\tau_3 - \tau_1 - \tau_3 + 2] + 1}{\sigma^2 + 4e^{2r}\sigma^4[\tau_1(1-\tau_2)\tau_3 - \tau_3 + 1]}\Big]. \end{aligned} \tag{36}$$

Optimization of Eq. (36) subject to a fixed photon number $\bar{N}$ at the senders' ends, i.e., $\bar{N} = \bar{n}_1 + \bar{n}_2 + \bar{n}_3 = 3\sinh^2 r + 4\sigma^2$ leads to the DC capacity of a network involving three senders and one receiver. With the aid of optimal conditions given by $\sigma^2 = \frac{3}{8}\sinh 2r$ and $r = (1/2)\ln(1 + \frac{2\bar{N}}{3})$, we obtain the capacity in terms of the photon strength of the senders and the state parameters as

$$\begin{aligned} C^{\mathcal{S}_1\mathcal{S}_2\mathcal{S}_3:\mathcal{R}}(\tau_1, \tau_2, \tau_3) &= \max_{\substack{\sigma \\ \bar{n}_1+\bar{n}_2=\bar{\mathcal{N}}}} \mathcal{I}(\mathcal{S}_1\mathcal{S}_2\mathcal{S}_3 : \mathcal{R}) \\ &= \frac{1}{2}\ln\left(\frac{1}{81}[\bar{N}(\bar{N}+3)+3][\bar{N}(\bar{N}+3)\tau_1(1-\tau_2)+3]\right) \\ &\quad + \frac{1}{2}\ln[([\bar{N}(\bar{N}+3)+3][3+\bar{N}(\bar{N}+3)(1-\tau_1)] + \bar{N}(\bar{N}+3)\tau_3\{[\bar{N}(\bar{N}+3)+3](\tau_1-1) - 3\tau_1\tau_2\})]. \end{aligned} \tag{37}$$

C. Classification of multimode states according to their DC capacities

Motivated from the three-mode results, let us first consider a symmetric situation, i.e., when $\tau_1 = \tau_2 = \tau_3 = 1/2$, the DC capacity becomes

$$C^{\mathcal{S}_1\mathcal{S}_2\mathcal{S}_3:\mathcal{R}}(1/2, 1/2, 1/2) = \tfrac{1}{2}\ln[[\bar{N}(\bar{N}+3)+3][\bar{N}(\bar{N}+3)+12]\{\bar{N}(\bar{N}+3)[2\bar{N}(\bar{N}+3)+27]+72\}] - \ln[36\sqrt{2}]. \tag{38}$$

Instead of equal τ_is, let us choose $\tau_1 = 1/3$, $\tau_2 = 1/4$, $\tau_3 = 4/5$, in which case the DC capacity reads as

$$C^{\mathcal{S}_1\mathcal{S}_2\mathcal{S}_3:\mathcal{R}}(1/3, 1/4, 4/5) = \tfrac{1}{2}\ln[[\bar{N}(\bar{N}+3)+3][\bar{N}(\bar{N}+3)+12]\{2\bar{N}(\bar{N}+3)[\bar{N}(\bar{N}+3)+24]+135\}] - \ln[18\sqrt{15}] \tag{39}$$

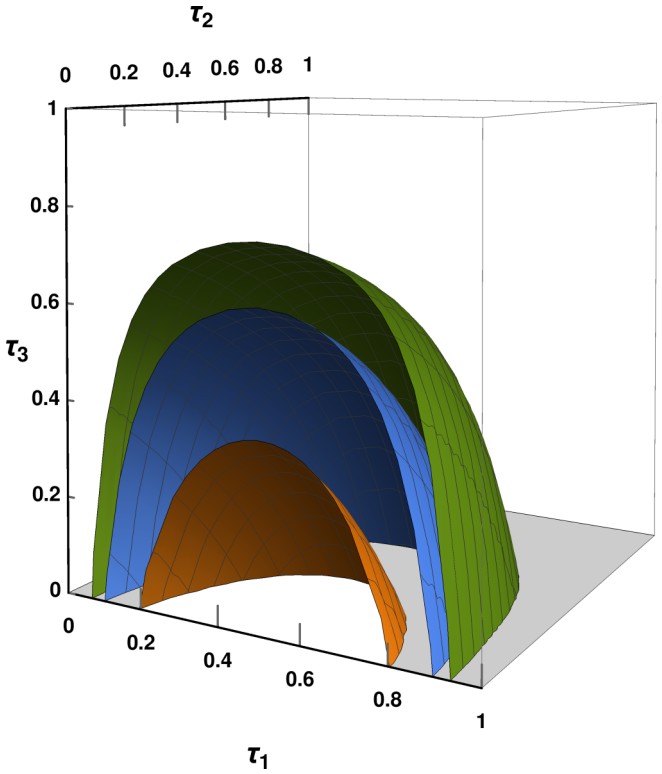

FIG. 4. Quantum advantage (in bits) in the DC scheme involving three senders and a single receiver in the state space characterized by τ_1 (x axis), τ_2 (y axis), and τ_3 (z axis). The orange, blue, and green planes represent $\bar{N} = 15$, $\bar{N} = 20$, and $\bar{N} = 25$, respectively. Note that the volume enclosed by the surfaces represents states which can provide quantum advantage, i.e., $\Delta^{\mathcal{S}_1\mathcal{S}_2\mathcal{S}_3:\mathcal{R}} > 0$. All the axes are dimensionless.

Comparing Eqs. (38) and (39), we find

$$C^{\mathcal{S}_1\mathcal{S}_2\mathcal{S}_3:\mathcal{R}}(1/2, 1/2, 1/2) > C^{\mathcal{S}_1\mathcal{S}_2\mathcal{S}_3:\mathcal{R}}(1/3, 1/4, 4/5).$$

To demonstrate it more explicitly, we vary τ_is and find the hierarchies among states which are beneficial for classical information transmission by using Eq. (37) with a fixed photon number $\bar{N}$ (see Fig. 4).

D. Outperforming quantum network with four-mode classical scheme

For the classical information transmission involving three senders and a single receiver without having any shared entangled state, the classical threshold reduces to

$$C_{cl}^{\mathcal{S}_1\mathcal{S}_2\mathcal{S}_3:\mathcal{R}} = 3(1 + \bar{N}/3)\ln(1 + \bar{N}/3) - 3(\bar{N}/3)\ln(\bar{N}/3). \tag{40}$$

Analyzing $\Delta^{\mathcal{S}_1\mathcal{S}_2\mathcal{S}_3:\mathcal{R}}$ in the τ_1, τ_2, τ_3 hyperplane, we observe that the quantum protocol can outperform the classical one for a given $\bar{N}$ as depicted in Fig. 4. The volume of states having quantum benefit increases with the increase of $\bar{N}$ as is also seen in the case of shared three-mode states and it is bounded by the surface in the figure. Moreover, we notice that all such favorable states are centered around $\tau_1 = 1/2$, which indicates that such a configuration is well suited for the proposed CVDC protocol between three senders and a single receiver. Furthermore, for small signal strength at the senders' end, states with small values of τ_2 and τ_3 are more helpful over the classical scheme compared to the states with high values of transmission coefficients of the beam splitters.

Like the three-mode entangled case, the solution of the equation, $C^{\mathcal{S}_1\mathcal{S}_2\mathcal{S}_3:\mathcal{R}}(\tau_1, \tau_2, \tau_3) = C_{cl}^{\mathcal{S}_1\mathcal{S}_2\mathcal{S}_3:\mathcal{R}}$ for $\bar{N}$ can give the threshold energy $\bar{N}_{th}^{\mathcal{S}_1\mathcal{S}_2\mathcal{S}_3:\mathcal{R}}(\tau_1, \tau_2, \tau_3)$ for the shared state comprising state parameters τ_1, τ_2, and τ_3, above which $\Delta^{\mathcal{S}_1\mathcal{S}_2\mathcal{S}_3:\mathcal{R}} > 0$. For example, $\bar{N}_{th}^{\mathcal{S}_1\mathcal{S}_2\mathcal{S}_3:\mathcal{R}}(1/2, 1/2, 1/2) = 24.87$ and

$$\bar{N}_{th}^{\mathcal{S}_1\mathcal{S}_2\mathcal{S}_3:\mathcal{R}}\Big|_{\min_{\{\tau_1,\tau_2,\tau_3\}}} = 11.45,$$

for the shared four-mode genuinely multimode entangled states. In this situation, let us identify the range of state parameters, i.e., τ_1, τ_2, and τ_3 for a given energy $\bar{N}$ so that the quantum advantage can be prevailed. They turn out to be

$$\tau_1\big|_{\substack{\max\\\min}} = 0.5 \pm \sqrt{\frac{9(\bar{N}(\bar{N}+3)+6)^2 - \frac{4\bar{N}^{-2\bar{N}}(\bar{N}+3)^{2\bar{N}+6}}{[\bar{N}(\bar{N}+3)+3]^2}}{36\bar{N}^2(\bar{N}+3)^2}}, \tag{41}$$

while for given $\bar{N}$ and τ_1,

$$\tau_2\big|_{\max} = \frac{\frac{(\bar{N}+3)^{2\bar{N}+6}\bar{N}^{-2\bar{N}}}{[\bar{N}(\bar{N}+3)+3]^2[\bar{N}(\bar{N}+3)(\tau_1-1)-3]} + 9(\bar{N}+3)\bar{N}\tau_1 + 27}{9\bar{N}(\bar{N}+3)\tau_1}. \tag{42}$$

When $\bar{N}$, τ_1, and τ_2 are fixed, the third transmission coefficient takes the form as

$$\tau_3\big|_{\max} = \frac{9[\bar{N}(\bar{N}+3)+3]^2[\bar{N}(\bar{N}+3)(\tau_1-1)-3][\bar{N}(\bar{N}+3)\tau_1(\tau_2-1)-3] - \bar{N}^{-2\bar{N}}(\bar{N}+3)^{2\bar{N}+6}}{9\bar{N}(\bar{N}+3)[\bar{N}(\bar{N}+3)+3][\bar{N}(\bar{N}+3)\tau_1(\tau_2-1)-3]\{[\bar{N}(\bar{N}+3)+3](\tau_1-1)-3\tau_1\tau_2\}}. \tag{43}$$

Substituting $\bar{N} = 3e^r \sinh r$ into Eqs. (37) and (40), we obtain $C^{\mathcal{S}_1\mathcal{S}_2\mathcal{S}_3:\mathcal{R}} \sim 8r$ and $C_{cl}^{\mathcal{S}_1\mathcal{S}_2\mathcal{S}_3:\mathcal{R}} \sim 6r$, respectively, for large r. Therefore, the ratio between the quantum and classical protocols for three senders and a single receiver becomes

$$\frac{C^{\mathcal{S}_1\mathcal{S}_2\mathcal{S}_3:\mathcal{R}}}{C_{cl}^{\mathcal{S}_1\mathcal{S}_2\mathcal{S}_3:\mathcal{R}}} = \frac{4}{3} \quad \text{(at large } r\text{)}. \tag{44}$$

In this case, the break-even squeezing strength of the quantum protocol, given in Eq. (38), required to defeat the classical threshold with the DC capacity for a given senders' photon number $\bar{N}$ reads $r^{\mathcal{S}_1\mathcal{S}_2\mathcal{S}_3:\mathcal{R}}_{\text{break}-\text{even}}(\tau_1 = \tau_2 = \tau_3 = 1/2) = 1.433$ which is 1.107 for the three-mode case with $\tau_1 = \tau_2 = 1/2$. It implies that the squeezing strength required to obtain improvement in the mentioned quantum protocol increases with the increase of the number of modes. Thus for the three senders-one receiver scenario, there is a quantum advantage beyond $r^{\mathcal{S}_1\mathcal{S}_2\mathcal{S}_3:\mathcal{R}}_{\text{break}-\text{even}}(\tau_1, \tau_2, \tau_3)$.

At this point, it can possibly be argued that, for $\mathcal{N}$ senders and a single receiver, the ratio between the capacities of the quantum and classical channels takes the form

$$\frac{C^{\mathcal{S}_1\mathcal{S}_2\mathcal{S}_3:\mathcal{R}}}{C^{\mathcal{S}_1\mathcal{S}_2\mathcal{S}_3:\mathcal{R}}_{cl}} = \frac{\mathcal{N}+1}{\mathcal{N}}, \tag{45}$$

at large r, where we used Eqs. (33) and (44) to present this conjecture.

V. CONCLUSION

In quantum communication, which includes both classical information transmission as well as quantum state transfer, shared entangled states are necessary to exhibit any quantum advantage. To transfer classical information, say two bits, the classical protocol where no shared entangled state is available requires four-dimensional objects for encoding while it reduces to a two-dimensional system with the help of shared entangled states, and hence the scheme is called dense coding (DC). In finite-dimensional systems, the capacity of dense coding for an arbitrary shared state is known when there are an arbitrary number of senders and a single or two receivers.

For continuous variable (CV) systems, since the dimension of the systems involved is infinite, the DC capacity can only be meaningful when it is obtained by fixing the amount of energy that can be sent from the sender to the receiver. Without this constraint, the capacity would simply diverge. Using this energy-constrained capacity, quantum advantage in CVDC was demonstrated for a single sender and a single receiver scenario [40].

In this work, we went beyond the single sender-receiver scenario and proposed a design for continuous variable DC network with multiple senders and a single receiver. In particular, we presented a possible blueprint of the encoding as well as decoding strategies, computed the corresponding classical energy-constrained capacities of a quantum channel, and optimum classical threshold, which can be achieved in the absence of a shared entangled state. We fixed the encoding strategies to be local displacement operations in the senders' side, while the decoding involves the use of beam splitters and the homodyne measurement of quadratures.

We demonstrated the efficacy of the CVDC network involving two as well as three senders and a single receiver when the shared states are the three- and four-mode states. In both cases, we showed that the quantum protocol can benefit over the classical one, thereby establishing the usefulness of multimode entangled states as resources. With the increase of energy, we found that the quantum advantage also got enhanced. Moreover, we computed the critical energy which is required for the successful implementation of CVDC with an entangled resource.

A practical communication technology demands the transfer of data among various nodes in a network. Hence the construction of the protocol presented here may shed light on establishing a network for transmitting classical information involving multiple nodes using squeezed states of light which can be implementable in laboratories.

ACKNOWLEDGMENTS

A.P., R.G., and A.S.D. acknowledge the support from the Interdisciplinary Cyber Physical Systems (ICPS) program of the Department of Science and Technology (DST), India, Grant No. DST/ICPS/QuST/Theme-1/2019/23. T.D. acknowledges support by the Foundation for Polish Science (IRAP project, ICTQT, contract no. MAB/2018/5, co-financed by EU within Smart Growth Operational Programme. This work has been partly supported by the Hong Kong Research Grant Council (RGC) through Grant No. 17300918.

[1] C. H. Bennett and G. Brassard, Theor. Comput. Sci. **560**, 7 (2014).
[2] A. K. Ekert, Phys. Rev. Lett. **67**, 661 (1991).
[3] T. Jennewein, C. Simon, G. Weihs, H. Weinfurter, and A. Zeilinger, Phys. Rev. Lett. **84**, 4729 (2000).
[4] N. Gisin, G. Ribordy, W. Tittel, and H. Zbinden, Rev. Mod. Phys. **74**, 145 (2002).
[5] U. Vazirani and T. Vidick, Phys. Rev. Lett. **113**, 140501 (2014).
[6] D. Mayers and A. Yao, *Proceedings 39th Annual Symposium on Foundations of Computer Science (Cat. No.98CB36280)* (IEEE, Piscataway, NJ, 1998), pp. 503–509.
[7] C. A. Miller and Y. Shi, J. ACM **63**, 1 (2016).
[8] C. H. Bennett and S. J. Wiesner, Phys. Rev. Lett. **69**, 2881 (1992).
[9] A. Sen(De) and U. Sen, Phys. News **40**, 17 (2010).
[10] N. Gisin and R. Thew, Nat. Photonics **1**, 165 (2007).
[11] R. Demkowicz-Dobrzański, A. Sen(De), U. Sen, and M. Lewenstein, Phys. Rev. A **80**, 012311 (2009).
[12] A. Sen(De), U. Sen, and M. Żukowski, Phys. Rev. A **68**, 032309 (2003).
[13] C. H. Bennett, G. Brassard, C. Crépeau, R. Jozsa, A. Peres, and W. K. Wootters, Phys. Rev. Lett. **70**, 1895 (1993).
[14] L. Vaidman, Phys. Rev. A **49**, 1473 (1994).
[15] S. L. Braunstein and H. J. Kimble, Phys. Rev. Lett. **80**, 869 (1998).
[16] R. Raussendorf and H. J. Briegel, Phys. Rev. Lett. **86**, 5188 (2001).
[17] H. J. Briegel and R. Raussendorf, Phys. Rev. Lett. **86**, 910 (2001).

[18] R. Raussendorf, D. E. Browne, and H. J. Briegel, Phys. Rev. A **68**, 022312 (2003).
[19] P. Walther, K. J. Resch, T. Rudolph, E. Schenck, H. Weinfurter, V. Vedral, M. Aspelmeyer, and A. Zeilinger, Nature (London) **434**, 169 (2005).
[20] R. Raussendorf, J. Harrington, and K. Goyal, New J. Phys. **9**, 199 (2007).
[21] R. Raussendorf and J. Harrington, Phys. Rev. Lett. **98**, 190504 (2007).
[22] F. Verstraete, M. M. Wolf, and C. J. Ignacio, Nat. Phys. **5**, 633 (2009).
[23] X. Ma, X. Yuan, Z. Cao, B. Qi, and Z. Zhang, npj Quantum Inf. **2**, 16021 (2016).
[24] C. Kollmitzer, S. Schaur, S. Rass, and B. Rainer, *Quantum Random Number Generation* (Springer, Cham, Germany, 1997).
[25] D. Bruß, G. M. D'Ariano, M. Lewenstein, C. Macchiavello, A. Sen(De), and U. Sen, Phys. Rev. Lett. **93**, 210501 (2004).
[26] D. Bruß, M. Lewenstein, A. Sen(De), U. Sen, G. M. D'Ariano, and C. Macchiavello, Int. J. Quantum. Inform. **4**, 415 (2006).
[27] T. Das, R. Prabhu, A. Sen(De), and U. Sen, Phys. Rev. A **92**, 052330 (2015).
[28] T. Das, R. Prabhu, A. Sen(De), and U. Sen, Phys. Rev. A **90**, 022319 (2014).
[29] R. Prabhu, A. K. Pati, A. Sen (De), and U. Sen, Phys. Rev. A **87**, 052319 (2013).
[30] J. Lee, S.-W. Ji, J. Park, and H. Nha, Phys. Rev. A **90**, 022301 (2014).
[31] L. Czekaj, J. K. Korbicz, R. W. Chhajlany, and P. Horodecki, Phys. Rev. A **82**, 020302(R) (2010).
[32] K. Boström and T. Felbinger, Phys. Rev. Lett. **89**, 187902 (2002).
[33] N. J. Beaudry, M. Lucamarini, S. Mancini, and R. Renner, Phys. Rev. A **88**, 062302 (2013).
[34] T. Das, K. Horodecki, and R. Pisarczyk, arXiv:2106.13310.
[35] H. Weinfurter, Europhys. Lett. **25**, 559 (1994).
[36] K. Mattle, H. Weinfurter, P. G. Kwiat, and A. Zeilinger, Phys. Rev. Lett. **76**, 4656 (1996).
[37] N. Lütkenhaus, J. Calsamiglia, and K.-A. Suominen, Phys. Rev. A **59**, 3295 (1999).
[38] D. Leibfried, R. Blatt, C. Monroe, and D. Wineland, Rev. Mod. Phys. **75**, 281 (2003).
[39] L. M. K. Vandersypen and I. L. Chuang, Rev. Mod. Phys. **76**, 1037 (2005).
[40] S. L. Braunstein and H. J. Kimble, Phys. Rev. A **61**, 042302 (2000).
[41] A. Einstein, B. Podolsky, and N. Rosen, Phys. Rev. **47**, 777 (1935).
[42] S. Hao, H. Shi, W. Li, J. H. Shapiro, Q. Zhuang, and Z. Zhang, Phys. Rev. Lett. **126**, 250501 (2021).
[43] S. Barzanjeh, S. Pirandola, and C. Weedbrook, Phys. Rev. A **88**, 042331 (2013).
[44] G. Adesso, S. Ragy, and A. R. Lee, Open Syst. Inf. Dyn. **21**, 1440001 (2014).
[45] M. S. Kim, J. Lee, and W. J. Munro, Phys. Rev. A **66**, 030301(R) (2002).
[46] H. Wang, Y. Pi, W. Huang, Y. Li, Y. Shao, J. Yang, J. Liu, C. Zhang, Y. Zhang, and B. Xu, Opt. Express **28**, 32882 (2020).
[47] T. C. Ralph and E. H. Huntington, Phys. Rev. A **66**, 042321 (2002).
[48] J. Jing, J. Zhang, Y. Yan, F. Zhao, C. Xie, and K. Peng, Phys. Rev. Lett. **90**, 167903 (2003).
[49] S. Barnett and P. Radmore, *Methods in Theoretical Quantum Optics* (Oxford Scholarship Online, Oxford, UK, 2002).
[50] E. Wigner, Phys. Rev. **40**, 749 (1932).
[51] A. Holevo, IEEE Trans. Inf. Theory **44**, 269 (1998).
[52] C. M. Caves and P. D. Drummond, Rev. Mod. Phys. **66**, 481 (1994).
[53] H. P. Yuen and M. Ozawa, Phys. Rev. Lett. **70**, 363 (1993).
[54] P. van Loock and S. L. Braunstein, Phys. Rev. Lett. **84**, 3482 (2000).
[55] G. Adesso, A. Serafini, and F. Illuminati, New J. Phys. **9**, 60 (2007).
[56] A. Adesso and F. Illuminati, J. Phys. A: Math. Theor. **40**, 7821 (2007).